

Identifying Black Hole Formation in Core-Collapse Supernova Simulations

Noah E. Wolfe,¹ Jonah M. Miller,² and Carla Fröhlich¹

¹*Department of Physics, North Carolina State University, Raleigh NC 27695 USA*

²*CCS-2, Computational Physics and Methods, Los Alamos National Laboratory, Los Alamos NM 87544 USA*

(Dated: December 2021)

I. INTRODUCTION

Core-collapse supernovae (CCSNe) are the deaths of massive stars $\gtrsim 8M_{\odot}$, which occur when the iron core in the center of these stars becomes too heavy to be supported by further nuclear burning. The inner regions of the star begin to contract under gravity, and the iron core is converted into neutrons through electron capture. Eventually, the core reaches the neutron degeneracy pressure, and reflects infalling material into an outward-expanding shockwave. In a successful explosion, this shockwave is able to gravitationally unbind the star, leaving behind the dense, neutronized iron core as a neutron star; in an unsuccessful explosion, it will fall back on the core, which collapses into a black hole. Thus, to properly understand these events requires at minimum general relativistic hydrodynamics, nuclear physics, and particle (neutrino) physics. As unique astrophysical laboratories, CCSNe connect to other astrophysical interests including stellar population modeling, galactic chemical evolution, and stellar evolution, as well as questions of fundamental physics like the nuclear equation of state and the origin of black holes. However, the observable products of CCSNe are indirect measures of astrophysical and physical questions due to the complex and highly-degenerate relationships between mechanism processes across physical scales. For example, a key CCSNe observable is the ejected Ni-56 mass, but this does not yield insight into microphysics like the nuclear equation of state [1]. Although the advent of multi-messenger astronomy, and especially the possibility of detecting gravitational wave emission from CCSNe, may ameliorate current observational deficiencies, we will still need accurate mappings between theoretical CCSNe frameworks and astronomical observation.

Currently, complex numerical models bridge this gap. In the past decade, CCSNe modeling has achieved important milestones, including successful explosions in both 2D (axially-symmetric) and 3D models, which incorporate directly or approximately many of the physics detailed above. However, high-dimensional (2D and 3D) models are significantly hampered by their computation time, requiring on the order of weeks or months to successfully evaluate. In recent years, 1D (spherically-symmetric) CCSNe modeling methods have addressed this gap, including the **PUSH** [2, 3] and **STIR** [4] methods. These models are physically-informed, while only requiring on the order of 8 hours to a few days to fully evaluate.

In this work, we focus **PUSH**, created in part by researchers at NC State. The **PUSH** method is implemented in the **ail_pdr** CCSNe simulation code, alongside the **AGILE** implicit general relativistic hydrodynamics code [5] and approximations to neutrino physics, to provide self-consistent modeling of CCSNe and prediction of multi-messenger observables (such as light emission and nucleosynthetic yields; [1, 6]). However, the computational advantage of spherically-symmetric code is somewhat hindered by its treatment of failed supernovae. In particular, when the shock falls back onto the dense core, the central density ρ_c of the star rises dramatically, approaching $\gtrsim 10^{15}\text{g/cm}^3$. Physically, we know black hole formation occurs as $\rho_c \rightarrow \infty$, and so heuristically a high central density in failed supernova models corresponds to black hole formation. Since numerical models cannot resolve infinite densities, **ail_pdr** crashes with floating point precision errors at these high densities approaching black hole formation.

To save on computational expense and improve our ability to differentiate from crashes involving black hole formation and other numerical singularities (or errors) in **ail_pdr**, and thus further enhance the research use of this code, we investigated a method of identifying black hole formation in advance of the **ail_pdr** crashing. We describe the type of event horizon we identify, the expansion H that characterizes horizon formation, and preliminary attempts to identify horizon formation.

II. SUPERNOVA METHODOLOGY

The **ail_pdr** code evolves progenitor models through collapse, bounce, and post-bounce, using the same methods as in [3], [7], and [8]. This method evolves progenitor models in spherical symmetric using the fully general relativistic, adaptive-mesh hydrodynamics code **AGILE** [5], with the Isotropic Diffusion Source Approximation (**IDSA**) for electron-flavor neutrino transport [9], and the Advanced Leakage Scheme (**ALS**) for heavy-flavor (muon and tau flavor) neutrino transport [10]. This scheme also relies on the **PUSH** method, which provides a physically-informed, self-consistent [6] means of driving spherically-symmetric (1D) models to explosion. The full methodology of **PUSH** is described in [2]

and [3], however in short, PUSH prescribes a deposition of heavy-flavor neutrino energy behind the supernova shock wave to imitate hydrodynamical heating effects that drive higher-dimensional models to explosion. We also specify a nuclear equation of state; in this case, the DD2 equation of state of [11].

Here, we focus on AGILE, as this is where the physics of general relativity are implemented in `ail_pdr`, and thus our entry point for identifying black hole formation. Much of this description can be found in Section 4 and Appendix 7 of [12]. The AGILE code solves a system of hydrodynamic equations F in a Lagrangian coordinate system that follows each parcel of fluid material, or as it is specifically implemented in `ail_pdr`, each zone. The full system of equations F is beyond the scope of this work, It does so with an implicit time step scheme; at each time t , AGILE records a “state vector” y that contains the relevant hydrodynamic quantities to be evolved, and solves for $\partial y/\partial t$ such that

$$F\left(t, y, \frac{\partial y}{\partial t}\right) = 0. \quad (1)$$

Numerically, this is expressed as solving

$$F(y^n, y^{n+1}, dt) = 0, \quad (2)$$

where n denotes the current timestep and $dt = t^{n+1} - t^n$ is determined by user-set restrictions on the timestep, and this system is solved for y^{n+1} via a Newton-Raphson scheme.

The AGILE code uses a coordinate system (t, a, θ, φ) , where t denotes the time, a is a spatial coordinate corresponding to the mass enclosed by a sphere at coordinate a , and θ, φ are the usual polar and axial angles. [12] defines a metric for AGILE which, from Appendix 7, is

$$ds^2 = -\alpha^2 dt^2 + \left(\frac{1}{\Gamma} \frac{\partial r}{\partial a}\right)^2 da^2 + r^2(a, t) d\Omega^2 \quad (3)$$

where $d\Omega^2 = d\theta^2 + \sin^2 \theta d\varphi^2$ is the standard solid angle element, α is the lapse function (which will be described in Section III A), r is the areal radius, and Γ is defined as,

$$\Gamma \equiv \sqrt{1 + u^2 - \frac{2m}{r}} \quad (4)$$

where the velocity $u \equiv (1/\alpha)^{-1} \partial r / \partial t$ and m is the gravitational rest mass.

III. NUMERICAL RELATIVITY

A. ADM 3+1 Formalism

In comparison to the AGILE metric presented in Equation 3, modern numerical relativity codes use the ADM metric. Conceptually, this metric divides coordinates in a “3+1” system of 3 spatial coordinates that define position on spatial hypersurfaces Σ , and a global time coordinate t . Generically, this metric is written as,

$$ds^2 = (-\alpha^2 + \beta_i \beta^i) dt^2 + 2\beta_i dt dx^i + \gamma_{ij} dx^i dx^j. \quad (5)$$

We note that we use the Einstein summation convention, where repeated indices (one lowered, one raised) indicate summation, as in

$$a_\mu b^\mu = \sum_\mu a_\mu b^\mu. \quad (6)$$

We will use Latin indices $(a, b, c, \dots, i, j, k, \dots)$ to denote spatial components of vectors and tensors, and Greek indices (μ, ν, \dots) to denote temporal + spatial components of vectors and tensors. In the ADM metric, α is the *lapse function*, defined as the change in proper time measured by observers moving perpendicular to the spatial hypersurfaces Σ ; these observers are known as Eulerian observers. Meanwhile, β^i is the *shift vector*, defined as the relative velocity between the Eulerian observers and spatial coordinate lines (lines of constant spatial coordinates). Figure 1, from [13], provides a helpful schematic representation of these values. The tensor γ_{ij} is the purely-spatial part of the full metric tensor $g_{\mu\nu}$, which we can read off from Equation 5 as,

$$g_{\mu\nu} = \begin{pmatrix} -\alpha^2 + \beta_k \beta^k & \beta_i \\ \beta_j & \gamma_{ij} \end{pmatrix}. \quad (7)$$

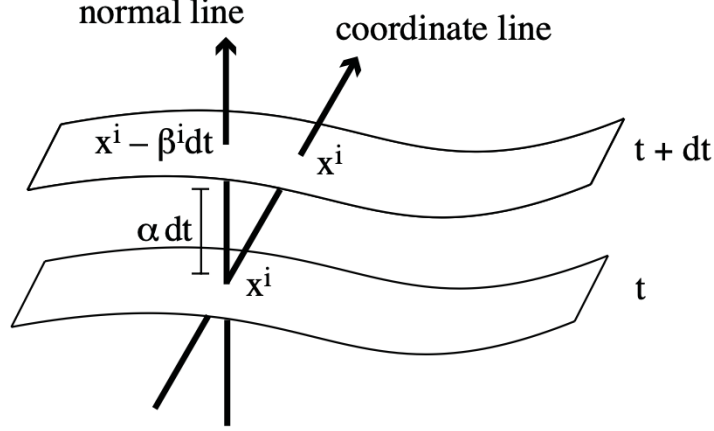


FIG. 1: Foliation of spacetime in the ADM 3+1 formalism. Each sheet is a spatial hypersurface Σ , and x_i are lines of constant spatial coordinates. The shift vector is denoted β^i , and the lapse is α , with a global time t .

Finally, we note that, in standard fashion, indices are raised and lowered using the relevant metric; either $g_{\mu\nu}$ for full 4-vectors or tensors with all 3 + 1 components, or γ_{ij} for vectors/tensors with only spatial components, for example,

$$\beta_i = \beta^i \gamma_{ij} \quad (8)$$

$$\beta^\mu = \beta_\mu g^{\mu\nu} \quad (9)$$

where $g^{\mu\nu}$ is the inverse of $g_{\mu\nu}$. We note that, at this stage, we have only defined a generic metric in the 3+1 formalism; later, we will specify this components in the case of **AGILE**.

B. Apparent Horizons and the Expansion

The most colloquially-known definition of a black hole is that of the event horizon, the point at which light cannot escape from a black hole. Formally, the event horizon encloses the region within which null geodesics (the paths light could take in a given spacetime) no longer converge towards infinity, and instead converge within the black hole. As a global definition however, it is difficult to work within in finite numerical codes.

The *apparent horizon* provides a local definition adjacent to that of the event horizon which can be evaluated on each spatial hypersurface Σ and indicates the existence of an event horizon; thus, it is well-suited to horizon identification in **ail_pdr**. Formally, an apparent horizon is found where the expansion H of null geodesics perpendicular to Σ is 0. As described by [13], the appearance of an apparent horizon implies the existence of an event horizon that is at least exterior to it, if not also coincident (under stricter assumptions).

Under the ADM formalism, in spherical symmetry, [13] gives us the expansion. In spherical symmetry, we have three spatial coordinates (r, θ, φ) , being the areal radius, polar angle, and axial angle, respectively, and a global time coordinate t . The spatial part of the metric, dl^2 , in spherical symmetry can be parameterized as,

$$dl^2 = A(r, t) dr^2 + r^2 B(r, t) d\Omega^2, \quad (10)$$

where $A(r, t)$ and $B(r, t)$ are functions determined by the particular spherically-symmetric spacetime that we are studying. Then, the expansion is given by [13] as,

$$H = \frac{1}{\sqrt{A(r, t)}} \left(\frac{2}{r} + \frac{\partial_r B(r, t)}{r} \right) - 2K_\theta^\theta, \quad (11)$$

where K_θ^θ is the $\theta\theta$ component of the extrinsic curvature tensor $K_{\mu\nu}$ with one index raised, and we introduce the shorthand notation $\partial_r \equiv \partial/\partial r$. As with $A(r, t)$, $B(r, t)$, the extrinsic curvature is a property of the particular spacetime that we investigate. Thus, to identify the formation of a black hole in our **ail_pdr** simulations, we calculate the expansion and find where $H = 0$.

IV. EXPANSION CALCULATION

To calculate the expansion in `ail_pdr` and cross-check our work, we took two approaches. In the first approach, we converted the `AGILE` metric into the ADM formalism and metric, providing $A(r, t)$, $B(r, t)$, and K_θ^θ so that we could then immediately apply Equation 11. In the second, we remained in the `AGILE` coordinate system and instead derived the expansion for the metric in Equation 3.

A. ADM Formalism

First, we convert the `AGILE` coordinate and metric system into ADM 3+1 spherically-symmetric coordinates of (t, r, θ, φ) . As defined by [12], in `AGILE` the coordinate r is partly a function of the mass coordinate a . So, we can write the total derivative dr as,

$$dr = \frac{1}{c_1} dt + \frac{1}{c_2} da, \quad (12)$$

where $(c_1)^{-1}, (c_2)^{-1}$ are constant, inverted to foreshadow the parallel expression of the total derivative of a ,

$$da = c_1 dt + c_2 da. \quad (13)$$

This skips many formal mathematical steps, but in practice we are allowed to perform this inversion because the Jacobian matrix that defines dr is simple and easily invertible. We also know, again from a deep formalism of real analysis that is beyond the scope of this work, that,

$$dr = \frac{\partial r}{\partial t} dt + \frac{\partial r}{\partial a} da. \quad (14)$$

Thus, and pulling the relevant derivatives from [12],

$$c_1 = \left(\frac{\partial r}{\partial t} \right)^{-1} = \frac{1}{\alpha u} \quad (15)$$

$$c_2 = \left(\frac{\partial r}{\partial a} \right)^{-1} = \frac{4\pi r^2 \rho}{\Gamma}, \quad (16)$$

where ρ is the rest mass density, $u \equiv \partial_t r / \alpha$, and Γ is defined in Equation 4. We substitute the total derivative da into the `AGILE` metric and get

$$\begin{aligned} ds^2 &= \left[-\alpha^2 + \left(\frac{1}{\Gamma} \frac{\partial r}{\partial a} c_1 \right)^2 \right] dt^2 + \left(\frac{1}{\Gamma} \frac{\partial r}{\partial a} c_2 \right)^2 dr^2 + 2 \left(\frac{1}{\Gamma} \frac{\partial r}{\partial a} \right)^2 c_1 c_2 dr dt + r^2 d\Omega^2 \\ ds^2 &= \left[-\alpha^2 + \left(\frac{1}{\Gamma} \frac{\partial r}{\partial a} \frac{1}{\alpha u} \right)^2 \right] dt^2 + \frac{1}{\Gamma^2} dr^2 + 2 \left(\frac{1}{\Gamma^2} \right) \left(\frac{\partial r}{\partial a} \right) \frac{1}{\alpha u} dr dt + r^2 d\Omega^2 \\ ds^2 &= \left[-\alpha^2 + (4\pi r^2 \rho \alpha u)^{-2} \right] dt^2 + \frac{1}{\Gamma^2} dr^2 + 2 (4\pi r^2 \rho \Gamma \alpha u)^{-1} dr dt + r^2 d\Omega^2 \end{aligned} \quad (17)$$

Now, this is in the form of a 3+1 metric, and we can identify the shift β_μ , and the coefficients $A(r, t), B(r, t)$ by inspection. We have,

$$\begin{aligned} 2\beta_r &= 2 \left(\frac{1}{\Gamma^2} \right) \left(\frac{\partial r}{\partial a} \right) \frac{1}{\alpha u}, \\ \therefore \beta_r &= \frac{1}{\alpha u} \frac{1}{\Gamma^2} \frac{\Gamma}{4\pi r^2 \rho} = (4\pi r^2 \rho \Gamma \alpha u)^{-1}, \end{aligned} \quad (18)$$

$$\therefore \beta_\mu = (0, \beta_r, 0, 0). \quad (19)$$

We can also identify, by inspecting this metric in relation to the purely-spatial parameterized spherically symmetric metric in Equation 10,

$$B(r, t) = 1, \quad (20)$$

$$A(r, t) = \frac{1}{\Gamma^2}. \quad (21)$$

Next, in order to calculate the expansion, we must compute the extrinsic curvature with one index raised and the other lowered. From [13], the extrinsic curvature is defined as,

$$K_{\mu\nu} = -(\nabla_\mu n_\nu + n_\mu n^\alpha \nabla_\alpha n_\nu) \quad (22)$$

$$K_{\nu\mu} = -(\nabla_\nu n_\mu + n_\nu n^\alpha \nabla_\alpha n_\mu) \quad (23)$$

where we permute the indices μ, ν in the second equation for aesthetic purposes in the rest of our calculation. We also recall, from PY 509 (General Relativity), that,

$$g^{\mu\sigma} \nabla_\alpha n_\sigma = \nabla_\alpha n^\mu, \quad (24)$$

so,

$$g^{\mu\sigma} K_{\nu\sigma} = -g^{\mu\sigma} (\nabla_\nu n_\sigma + n_\nu n^\alpha \nabla_\alpha n_\sigma) \quad (25)$$

$$= -(\nabla_\nu n^\mu + n_\nu n^\alpha \nabla_\alpha n^\mu) \quad (26)$$

$$= K_\nu^\mu. \quad (27)$$

From [13], the vector n_μ is the unit normal vector to the spatial hypersurfaces Σ , and is defined as such that,

$$n_\mu = (-\alpha, 0, 0, 0) \quad (28)$$

$$n^\mu = \frac{1}{\alpha} (1, -\beta_r, -\beta_\theta, -\beta_\varphi) \quad (29)$$

With the definition of β_μ in Equation 19, we use Mathematica to compute the $\theta\theta$ component of the extrinsic curvature with one index raised and the other lowered according to Equation 26 in terms of our hydrodynamic/general relativistic variables r, u, ρ, Γ , and α , yielding,

$$K_\theta^\theta = \frac{1}{4\pi r^3 \rho \alpha^2 u \Gamma} \quad (30)$$

Thus, the expansion in AGILE converted to the 3+1 formalism is,

$$\begin{aligned} H &= \frac{1}{\sqrt{A(r, t)}} \left(\frac{2}{r} + \frac{\partial_r B(r, t)}{r} \right) - 2K_\theta^\theta \\ &= \frac{1}{\sqrt{\Gamma^{-2}}} \left(\frac{2}{r} + \frac{\partial_r 0}{r} \right) - \frac{2}{4\pi r^3 \rho \alpha^2 u \Gamma} \\ \therefore H &= \frac{2\Gamma}{r} - \frac{1}{2\pi r^3 \rho \alpha^2 u \Gamma} \end{aligned} \quad (31)$$

B. AGILE Metric

In our second approach, we re-derive the expansion in AGILE's coordinate system. From equation 6.7.3 of [13], the expansion is

$$H = -\frac{1}{2} h^{\mu\nu} (\mathcal{L}_{\vec{s}} h_{\mu\nu} + \mathcal{L}_{\vec{n}} h_{\mu\nu}), \quad (32)$$

where \vec{s} is a free parameter, which is a unit normal vector with respect to the a two-dimensional surface embedded in the three-dimensional spacelike hypersurface Σ , \vec{n} is the timelike unit normal vector with respect to Σ , and $h_{\mu\nu}$ is defined as (in equation 6.7.2 of [13]),

$$h_{\mu\nu} = g_{\mu\nu} + n_\mu n_\nu - s_\mu s_\nu. \quad (33)$$

In AGILE's coordinate system, we are given the lapse α . The shift vector $\beta^i = 0$ as AGILE's coordinate system is Lagrangian; β^i is the relative velocity between an Eulerian observer and lines of constant spatial coordinates, but in a Lagrangian system where the coordinates follow each parcel of material, our observers are always at constant spatial coordinates. We also note that, from Appendix 7 of [13], the metric $g_{\mu\nu}$ is

$$g_{\mu\nu} = \begin{pmatrix} -\alpha^2 & 0 & 0 & 0 \\ 0 & \left(\frac{r'}{\Gamma}\right)^2 & 0 & 0 \\ 0 & 0 & r^2 & 0 \\ 0 & 0 & 0 & r^2 \sin^2 \theta \end{pmatrix}. \quad (34)$$

With $\beta^i = 0$, our vector \vec{n} is

$$n_\mu = (-\alpha, 0, 0, 0), \quad n^\mu = (1/\alpha, 0, 0, 0). \quad (35)$$

Additionally, since \vec{s} is a free parameter, we give it the form $(0, s, 0, 0)$, so that it will be perpendicular to the $(\theta, \varphi) = (0, 0)$ surface pointing in the $+a$ direction. We need \vec{s} to have unit length, i.e.

$$s^\mu g_{\mu\nu} s^\nu = 1, \quad (36)$$

$$\therefore s^a g_{aa} s^a = 1, \text{ as } g_{\mu\nu} \text{ is diagonal and only } s^a \neq 0, \quad (37)$$

$$\therefore s \left(\frac{r'}{\Gamma} \right)^2 s = 1, \quad (38)$$

$$\therefore s = \frac{\Gamma}{r'}, \text{ taking } + \text{ in the square root to } \vec{s} \text{ points in } +a. \quad (39)$$

Having specified s^μ , we can easily determine s_μ ,

$$s_\mu = g_{\mu\nu} s^\nu$$

$$\therefore s_t = g_{t\nu} s^\nu = 0 \quad (40)$$

$$s_a = g_{a\nu} s^\nu = g_{aa} s^a = \frac{1}{s^2} s = \frac{1}{s} \quad (41)$$

$$s_\theta = g_{\theta\nu} s^\nu = g_{\theta\theta} s^\theta = 0 \quad (42)$$

$$s_\varphi = g_{\varphi\nu} s^\nu = g_{\varphi\varphi} s^\varphi = 0. \quad (43)$$

So, with $g_{\mu\nu}$, n_μ , and s_μ in hand,

$$\begin{aligned} h_{\mu\nu} &= \begin{pmatrix} -\alpha^2 & 0 & 0 & 0 \\ 0 & s^{-2} & 0 & 0 \\ 0 & 0 & r^2 & 0 \\ 0 & 0 & 0 & r^2 \sin^2 \theta \end{pmatrix} + \begin{pmatrix} \alpha^2 & 0 & 0 & 0 \\ 0 & 0 & 0 & 0 \\ 0 & 0 & 0 & 0 \\ 0 & 0 & 0 & 0 \end{pmatrix} - \begin{pmatrix} 0 & 0 & 0 & 0 \\ 0 & s^{-2} & 0 & 0 \\ 0 & 0 & 0 & 0 \\ 0 & 0 & 0 & 0 \end{pmatrix} \\ \therefore h_{\mu\nu} &= \begin{pmatrix} 0 & 0 & 0 & 0 \\ 0 & 0 & 0 & 0 \\ 0 & 0 & r^2 & 0 \\ 0 & 0 & 0 & r^2 \sin^2 \theta \end{pmatrix} \end{aligned} \quad (44)$$

Using Mathematica, we raise both indices to also find,

$$h^{\mu\nu} = \begin{pmatrix} 0 & 0 & 0 & 0 \\ 0 & 0 & 0 & 0 \\ 0 & 0 & r^{-2} & 0 \\ 0 & 0 & 0 & r^{-2} \csc^2 \theta \end{pmatrix} \quad (45)$$

With $h_{\mu\nu}$, $h^{\mu\nu}$, n^μ , s^μ , we can now calculate the expansion. First, we calculate the two Lie derivatives; from the definition of the Lie derivative in terms of partial derivatives from [14] Exercise 21.5 (b), we have,

$$\begin{aligned} \mathcal{L}_{\vec{s}} h_{\mu\nu} &= s^\sigma \partial_\sigma h_{\mu\nu} + h_{\sigma\nu} \partial_\mu s^\sigma + h_{\mu\sigma} \partial_\nu s^\sigma, \\ &= s^a \partial_a h_{\mu\nu} + h_{a\nu} \partial_\mu s^a + h_{\mu a} \partial_\nu s^a, \\ &= s \partial_a h_{\mu\nu} + h_{a\nu} \partial_\mu s + h_{\mu a} \partial_\nu s, \end{aligned} \quad (46)$$

where, since only the $\theta\theta$ and $\varphi\varphi$ components of $h_{\mu\nu}$ are non-zero, those are the only terms of $\mathcal{L}_{\vec{s}}h_{\mu\nu}$ which may be non-zero. Recalling that $s = \Gamma/r' \equiv \Gamma/\partial_a r$, those terms are

$$\begin{aligned}\mathcal{L}_{\vec{s}}h_{\theta\theta} &= s\partial_a h_{\theta\theta} + \cancel{h_{a\theta}}^0 \partial_\theta s + \cancel{h_{\theta a}}^0 \partial_\theta s \\ &= s\partial_a r^2 \\ &= 2sr\partial_a r \\ &= 2r\frac{\Gamma}{r'}\partial_a r \\ &= 2r\Gamma\end{aligned}\tag{47}$$

$$\begin{aligned}\mathcal{L}_{\vec{s}}h_{\varphi\varphi} &= s\partial_a h_{\varphi\varphi} + \cancel{h_{a\varphi}}^0 \partial_\varphi s + \cancel{h_{\varphi a}}^0 \partial_\varphi s \\ &= s\partial_a r^2 \sin^2 \theta \\ &= 2sr \sin^2 \theta \partial_a r \\ &= 2r \sin^2 \theta \frac{\Gamma}{r'} \partial_a r \\ &= 2r\Gamma \sin^2 \theta.\end{aligned}\tag{48}$$

Similarly, with n^μ ,

$$\begin{aligned}\mathcal{L}_{\vec{n}}h_{\mu\nu} &= n^\sigma \partial_\sigma h_{\mu\nu} + h_{\sigma\nu} \partial_\mu n^\sigma + h_{\mu\sigma} \partial_\nu n^\sigma \\ &= n^t \partial_t h_{\mu\nu} + h_{t\nu} \partial_\mu n^t + h_{\mu t} \partial_\nu n^t\end{aligned}\tag{49}$$

$$(50)$$

with, as for $\mathcal{L}_{\vec{s}}h_{\mu\nu}$, since $h_{\mu\nu}$ is diagonal with $h_{aa} = 0$, the only non-zero terms are

$$\begin{aligned}\mathcal{L}_{\vec{n}}h_{\theta\theta} &= n^t \partial_t h_{\theta\theta} + \cancel{h_{t\theta}}^0 \partial_\theta n^t + \cancel{h_{\theta t}}^0 \partial_\theta n^t \\ &= \frac{1}{\alpha} \partial_t r^2 \\ &= \frac{2r}{\alpha} \partial_t r\end{aligned}\tag{51}$$

$$\begin{aligned}\mathcal{L}_{\vec{n}}h_{\varphi\varphi} &= n^t \partial_t h_{\varphi\varphi} + \cancel{h_{t\varphi}}^0 \partial_\varphi n^t + \cancel{h_{\varphi t}}^0 \partial_\varphi n^t \\ &= \frac{1}{\alpha} \partial_t r^2 \sin^2 \theta \\ &= \frac{2r \sin^2 \theta}{\alpha} \partial_t r\end{aligned}\tag{52}$$

With $h^{\mu\nu}$, $\mathcal{L}_{\vec{s}}h_{\mu\nu}$, and $\mathcal{L}_{\vec{n}}h_{\mu\nu}$, the expansion in AGILE coordinates becomes,

$$\begin{aligned}H &= -\frac{1}{2}h^{\mu\nu} (\mathcal{L}_{\vec{s}}h_{\mu\nu} + \mathcal{L}_{\vec{n}}h_{\mu\nu}) \\ &= -\frac{1}{2} [h^{\theta\theta} (\mathcal{L}_{\vec{s}}h_{\theta\theta} + \mathcal{L}_{\vec{n}}h_{\theta\theta}) + h^{\varphi\varphi} (\mathcal{L}_{\vec{s}}h_{\varphi\varphi} + \mathcal{L}_{\vec{n}}h_{\varphi\varphi})] \\ &= -\frac{1}{2} \left[\frac{1}{r^2} \left(2r\Gamma + \frac{2r\partial_t r}{\alpha} \right) + \frac{1}{r^2 \sin^2 \theta} \left(2r\Gamma \sin^2 \theta + \frac{2r \sin^2 \theta \partial_t r}{\alpha} \right) \right] \\ &= -\left(\frac{2\Gamma}{r} + \frac{2\partial_t r}{r\alpha} \right) \\ &= -\frac{2}{r} \left(\Gamma + \frac{\partial_t r}{\alpha} \right)\end{aligned}\tag{53}$$

Our condition for the appearance of an apparent horizon is that $H = 0$; in AGILE, this then reduces to the condition that, recalling from [12], $u \equiv \dot{r}/\alpha$,

$$\Gamma + \frac{\partial_t r}{\alpha} = 0\tag{54}$$

$$\therefore \Gamma + u = 0\tag{55}$$

or, equivalently,

$$\alpha\Gamma + \partial_t r = 0. \quad (56)$$

V. RESULTS

Using both of the approaches outlined in Section IV, we calculated the expansion in each zone, at various timesteps, during the collapse of two progenitors: *s15.0*, an exploding $15M_\odot$ solar metallicity progenitor, and *s22.2*, a failed (black hole forming) $22.2M_\odot$ solar metallicity progenitor.

A. ADM Formalism

Using our first approach, we calculate the expansion in each zone of both progenitors at a pre-bounce timestep, an immediately post-bounce timestep, and a late timestep, near the end of each simulation. These results are shown in Figures 2, 3, and 4, respectively. We note that in these figures the shock radius, plotted in orange, appears somewhat coincident with zero-crossings in the expansion, but not exactly so. The main issues that we observe is the large amount of crossings in the outer zones of the star at late times; we do not expect such crossings to occur as horizons should instead form deep within the star.

B. AGILE Metric

Using the second approach, we again calculated the expansion in each zone of both progenitors at a pre-bounce timestep, an immediately post-bounce timestep, and a late timestep, near the end of each simulation. These results are shown in Figures 5, 6, and 7, respectively. We note that in these calculations, the shock radius is no longer coincident with zero-crossings, but instead, small peaks in the expansion, which is not concerning. However, we still note that there are crossings at late times in the out zones of the star, which is unexpected.

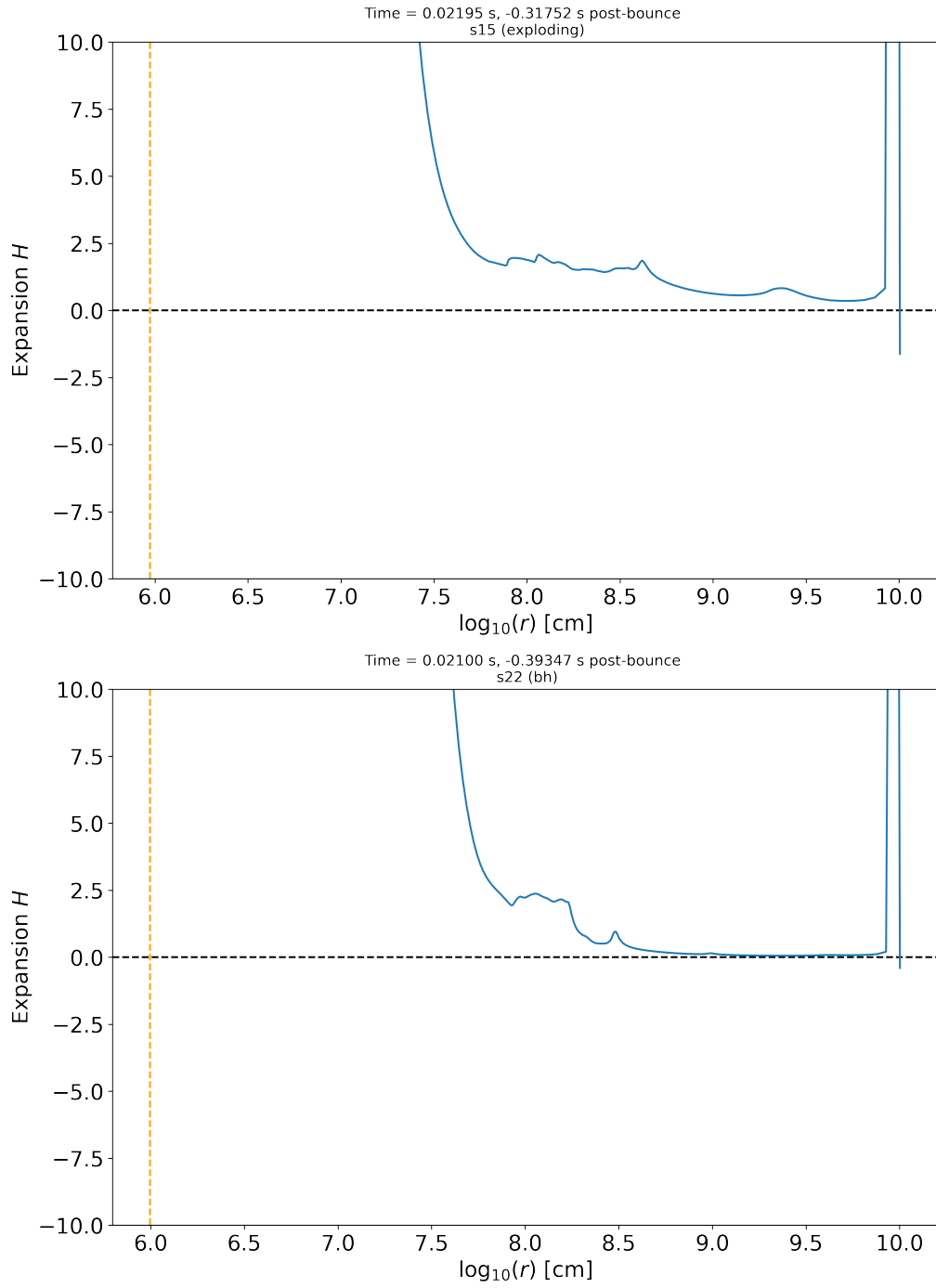


FIG. 2: Expansion calculated in the ADM formalism pre-bounce. Blue denotes the expansion, and the orange dashed line denotes the shock radius at that timestep.

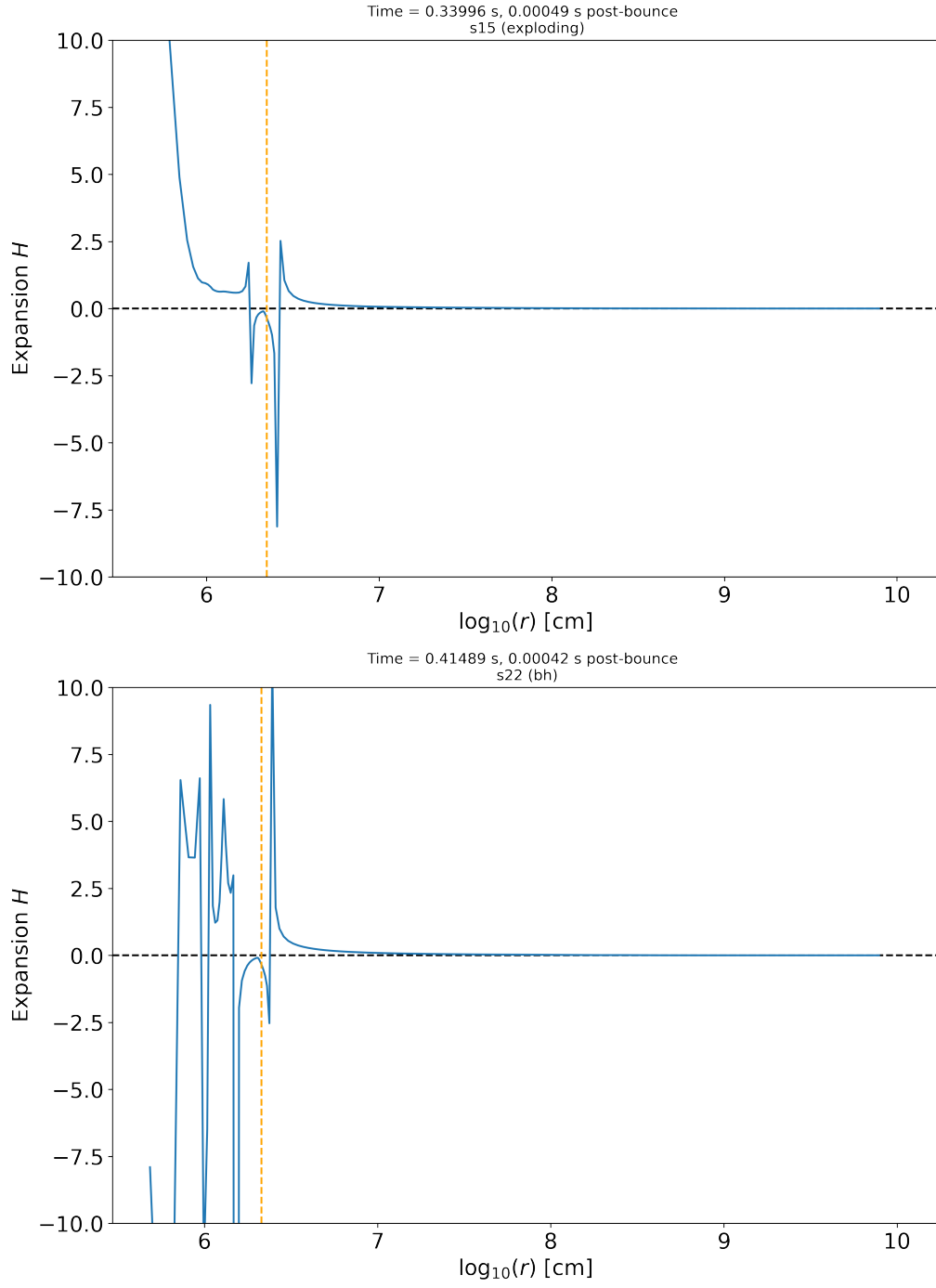


FIG. 3: Expansion calculated in the ADM formalism immediately post-bounce. Blue denotes the expansion, and the orange dashed line denotes the shock radius at that timestep.

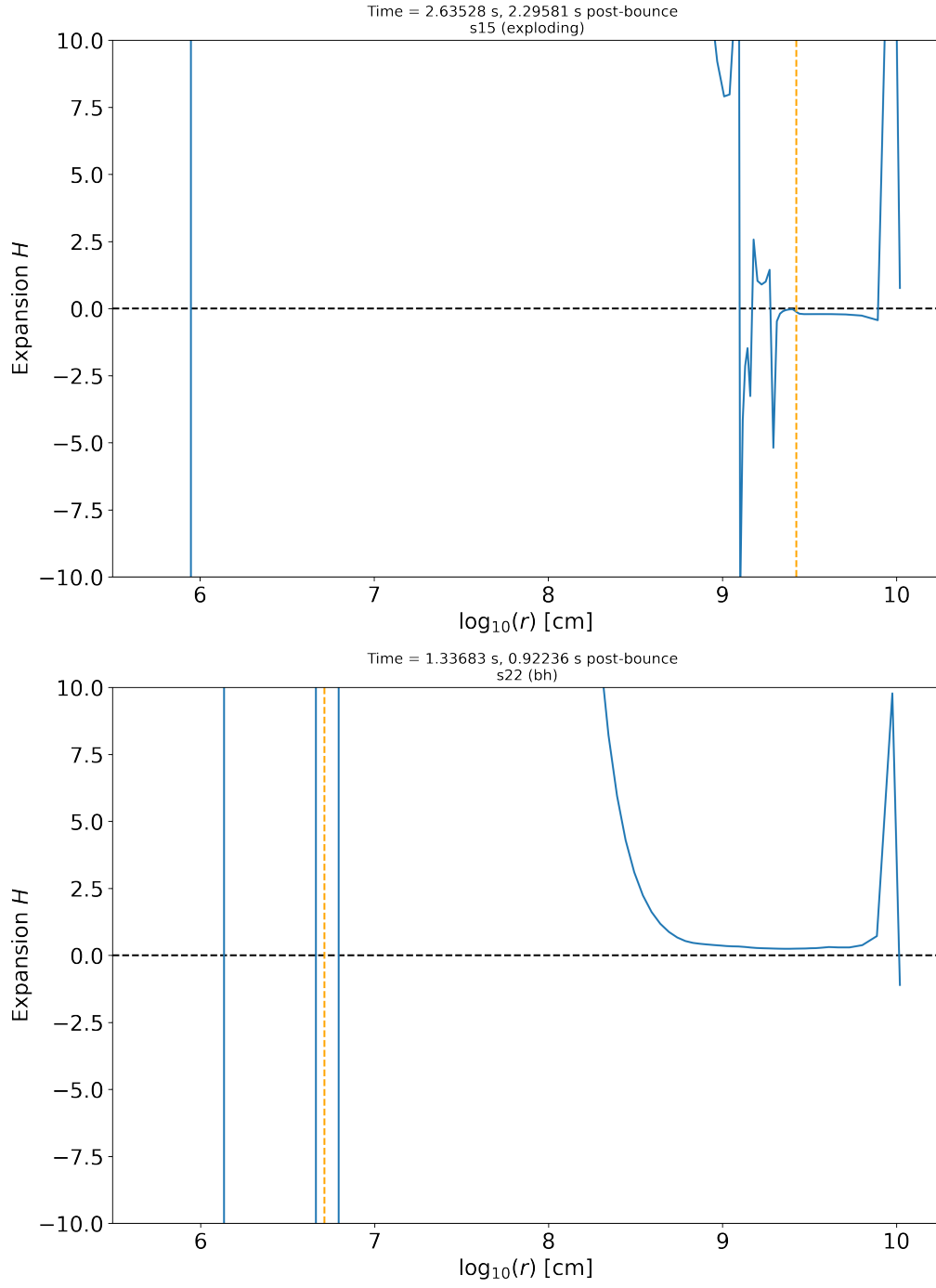


FIG. 4: Expansion calculated in the ADM formalism at late simulation times. Blue denotes the expansion, and the orange dashed line denotes the shock radius at that timestep.

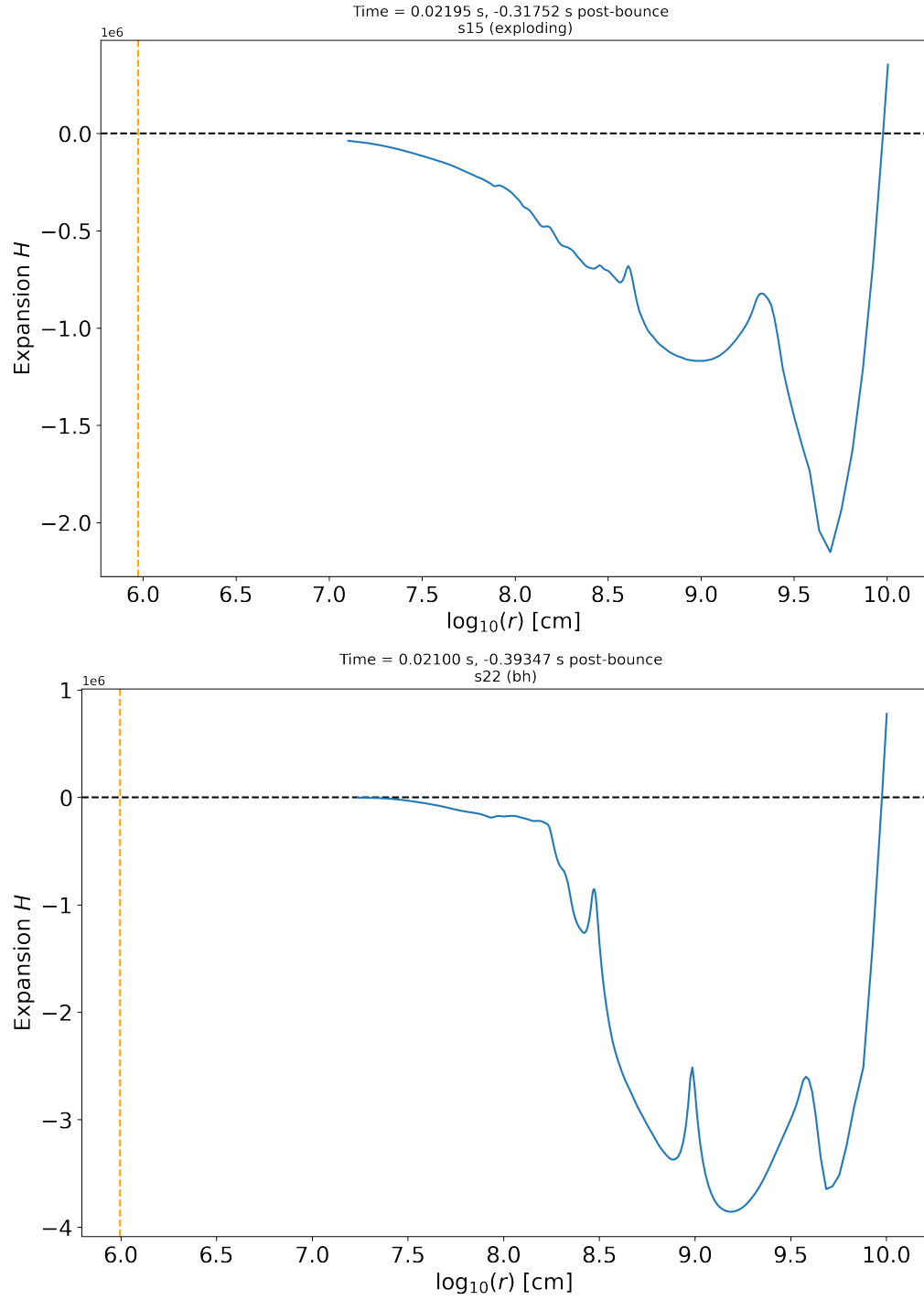


FIG. 5: Expansion calculated in AGILE coordinates pre-bounce. Blue denotes the expansion, and the orange dashed line denotes the shock radius at that timestep.

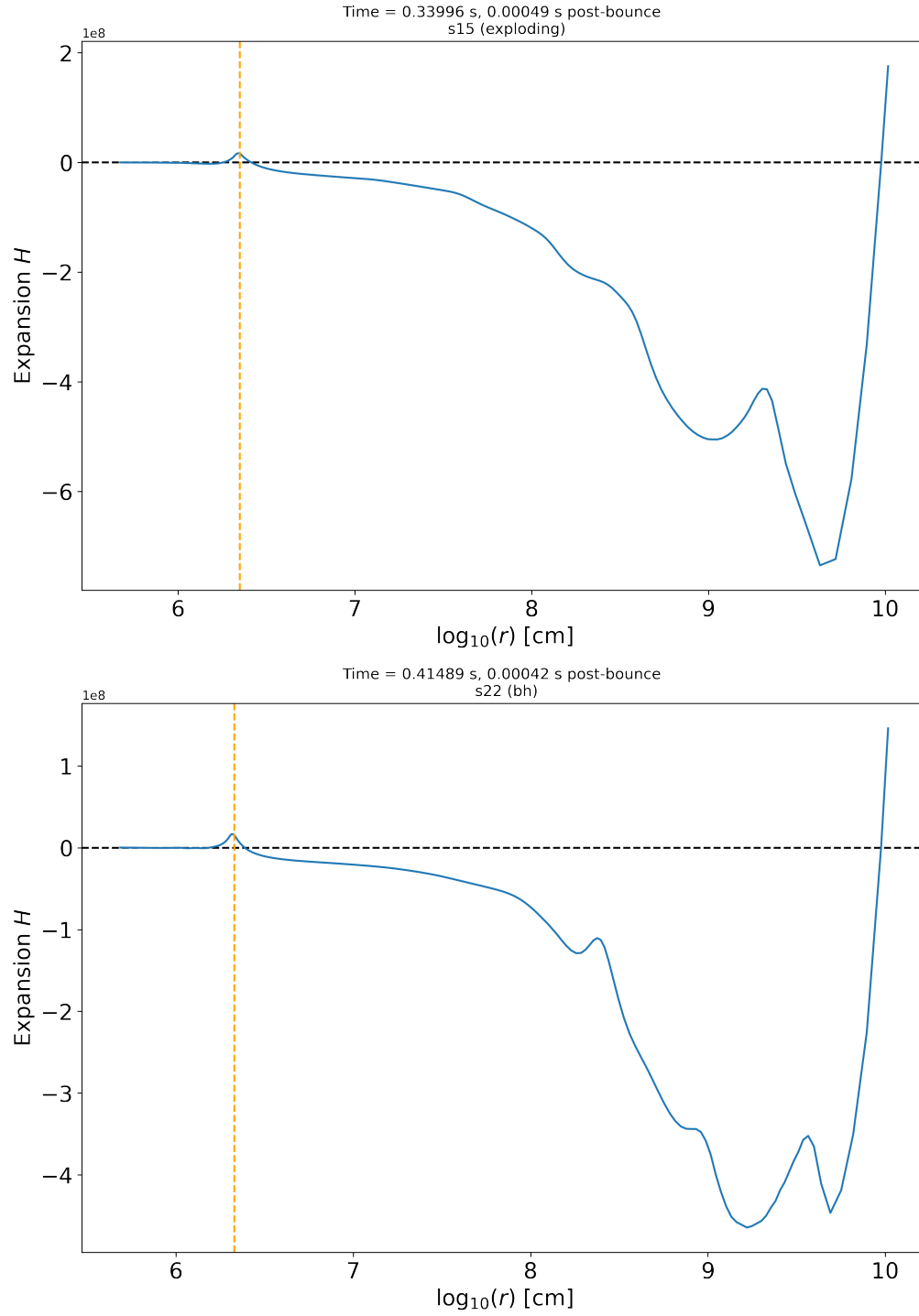


FIG. 6: Expansion calculated in AGILE coordinates immediately post-bounce. Blue denotes the expansion, and the orange dashed line denotes the shock radius at that timestep.

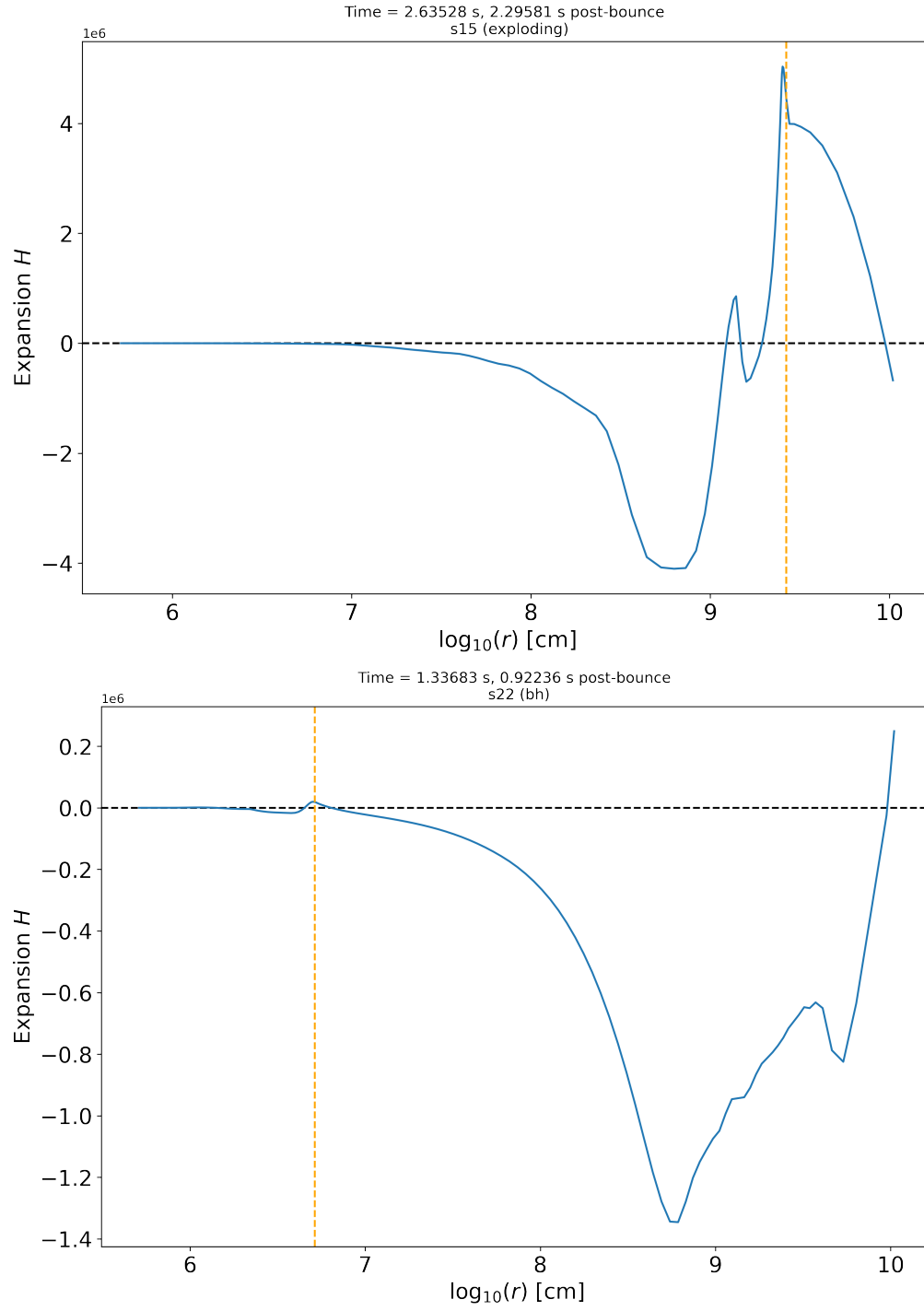


FIG. 7: Expansion calculated in AGILE coordinates at late simulation times. Blue denotes the expansion, and the orange dashed line denotes the shock radius at that timestep.

-
- [1] Somdutta Ghosh, Noah Wolfe, and Carla Fröhlich. PUSHing core-collapse supernovae to explosions in spherical symmetry V: Equation of state dependency of explosion properties, nucleosynthesis yields, and compact remnants. *arXiv e-prints*, art. arXiv:2107.13016, July 2021.
 - [2] A. Perego, M. Hempel, C. Fröhlich, K. Ebinger, M. Eichler, J. Casanova, M. Liebendörfer, and F.-K. Thielemann. PUSHing Core-collapse Supernovae to Explosions in Spherical Symmetry I: the Model and the Case of SN 1987A. *Astrophys. J.*, 806:275, June 2015. doi:10.1088/0004-637X/806/2/275.
 - [3] K. Ebinger, S. Curtis, C. Fröhlich, M. Hempel, A. Perego, M. Liebendörfer, and F.-K. Thielemann. PUSHing Core-collapse Supernovae to Explosions in Spherical Symmetry. II. Explodability and Remnant Properties. *Astrophys. J.*, 870:1, January 2019. doi:10.3847/1538-4357/aae7c9.
 - [4] Sean M. Couch, MacKenzie L. Warren, and Evan P. O'Connor. Simulating Turbulence-aided Neutrino-driven Core-collapse Supernova Explosions in One Dimension. *Astrophys. J.*, 890(2):127, February 2020. doi:10.3847/1538-4357/ab609e.
 - [5] M. Liebendörfer, S. Rosswog, and F.-K. Thielemann. An Adaptive Grid, Implicit Code for Spherically Symmetric, General Relativistic Hydrodynamics in Comoving Coordinates. , 141:229–246, July 2002. doi:10.1086/339872.
 - [6] Sanjana Curtis, Noah Wolfe, Carla Fröhlich, Jonah M. Miller, Ryan Wollaeger, and Kevin Ebinger. Core-Collapse Supernovae: From Neutrino-Driven 1D Explosions to Light Curves and Spectra. *arXiv e-prints*, art. arXiv:2008.05498, August 2020.
 - [7] S. Curtis, K. Ebinger, C. Fröhlich, M. Hempel, A. Perego, M. Liebendörfer, and F.-K. Thielemann. PUSHing Core-collapse Supernovae to Explosions in Spherical Symmetry. III. Nucleosynthesis Yields. *Astrophys. J.*, 870:2, January 2019. doi:10.3847/1538-4357/aae7d2.
 - [8] Kevin Ebinger, Sanjana Curtis, Somdutta Ghosh, Carla Fröhlich, Matthias Hempel, Albino Perego, Matthias Liebendörfer, and Friedrich-Karl Thielemann. PUSHing Core-collapse Supernovae to Explosions in Spherical Symmetry. IV. Explodability, Remnant Properties, and Nucleosynthesis Yields of Low-metallicity Stars. *Astrophys. J.*, 888(2):91, January 2020. doi:10.3847/1538-4357/ab5dcb.
 - [9] M. Liebendörfer, S. C. Whitehouse, and T. Fischer. The Isotropic Diffusion Source Approximation for Supernova Neutrino Transport. *Astrophys. J.*, 698:1174–1190, June 2009. doi:10.1088/0004-637X/698/2/1174.
 - [10] A. Perego, R. M. Cabezón, and R. Käppeli. An Advanced Leakage Scheme for Neutrino Treatment in Astrophysical Simulations. , 223:22, April 2016. doi:10.3847/0067-0049/223/2/22.
 - [11] M. Hempel and J. Schaffner-Bielich. A statistical model for a complete supernova equation of state. *Nuclear Physics A*, 837:210–254, June 2010. doi:10.1016/j.nuclphysa.2010.02.010.
 - [12] Matthias Liebendörfer. *Consistent modeling of core-collapse supernovae in spherically symmetric relativistic space-time*. PhD thesis, University of Basel, Switzerland, January 2000.
 - [13] Jörg Frauendiener. Miguel Alcubierre: Introduction to 3 + 1 numerical relativity. Oxford University Press, 2008, 464 pp., GBP63.50 ISBN-10: 0199205671, ISBN-13: 978-0199205677. *General Relativity and Gravitation*, 43(10):2931–2933, October 2011. doi:10.1007/s10714-011-1195-5.
 - [14] Charles W. Misner, Kip S. Thorne, and John A. Wheeler. *Gravitation*. 1973.